

Quasi-shear mode excitation of c-axis tilted MgZnO epitaxial thin film

Hiroki Kishi^{1,2†} and Takahiko Yanagitani^{1,2,3,4}

(¹Waseda Univ.; ²ZAIKEN; ³JST-CREST; ⁴JST-FOREST)

1. Introduction

Thickness shear mode piezoelectric thin films with high electromechanical coupling coefficient $k'_{35}{}^2$ are attractive for quasi-shear mode FBAR and SH-SAW devices.¹⁻⁵ As shown in **Fig. 1**, the single crystalline ZnO film with 28° tilt to the substrate normal has high k'_{35} . In 2007, our group fabricated polycrystalline ZnO films with a 23° tilt to the substrate normal and reported $k'_{35}{}^2 = 6.8\%$.⁶ However, this method requires the substrate to be placed perpendicular to the cathode. Therefore, the c-axis tilt angle and film thickness vary in the substrate. It is therefore difficult to grow c-axis tilted films on a large-size wafer for mass production. In addition, a dispersion of crystalline orientation in polycrystalline films is the disadvantage compared to the single crystals. It is preferable to fabricate epitaxial thin films with uniform tilt angle and film thickness over the entire substrate surface, by using standard planar sputtering machine.

- Thickness extensional mode $k_{33}{}^2$
- Thickness shear mode $k_{35}{}^2$

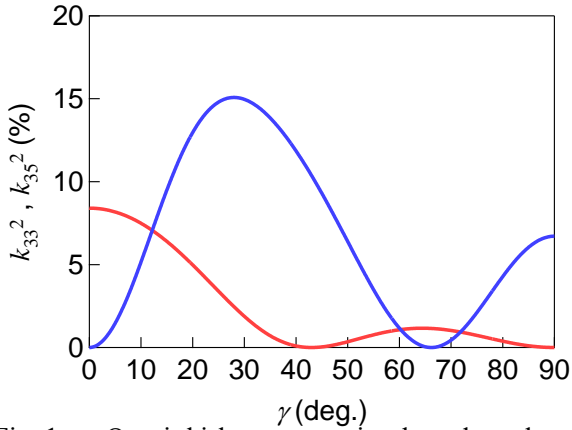


Fig. 1 Quasi-thickness extensional mode and quasi-thickness shear mode electromechanical coupling k^2 as a function of tilt angle in ZnO.

Our group previously reported that Mg-substituted ZnO significantly improves thickness extensional mode $k_t{}^2$.⁷

In this study, we fabricated c-axis tilted epitaxial MgZnO films by RF magnetron sputtering on a c-plane sapphire substrate with a 20° off-angle to the a-plane direction. Their quasi-shear mode $k'_{35}{}^2$ are extracted from shear wave conversion loss of the HBAR.

2. Fabricating process

(0001) Mg₃₀Zn₇₀O on (111) Pt films were grown on off-angle c-plane sapphire substrate by RF magnetron sputtering. The sapphire substrates were annealed at 1400°C in air before the growth.

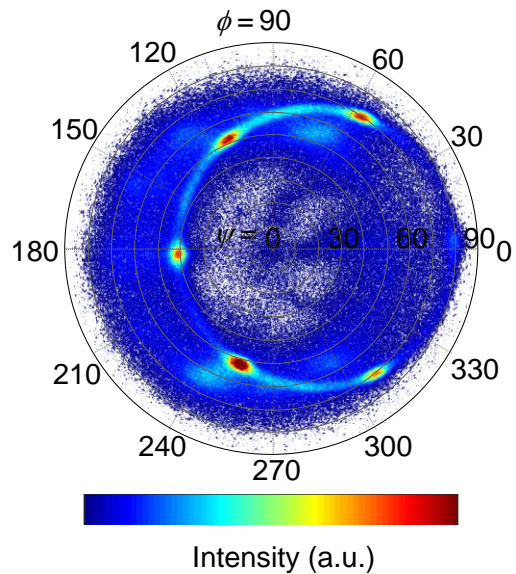
Table. I Growth condition of thin films

	Pt	MgZnO
RF power	80W	150W
Ar / O ₂	Ar 100%	15
Substrate - target distance	25mm	30mm
Size of target	2inch	4inch
Gas pressure	0.4Pa	0.5Pa
Deposition time	1min	1.5hour

3. Crystalline orientation

The crystalline orientation of the fabricated sample was examined by XRD. As shown in **Fig. 2**, in-plane six-fold symmetry which is shifted 20° to the right is observed. This indicates that the MgZnO thin film is epitaxially grown reflecting the 20° off-angle of the substrate. FWHM of χ and ϕ scan (0001) MgZnO rocking curves were 4.7° and 5.5° respectively, which shows excellent in-plane and out-of-plane orientation.

(a)



e-mail:

1. hiroki3141592@akane.waseda.jp
2. yanagitani@waseda.jp

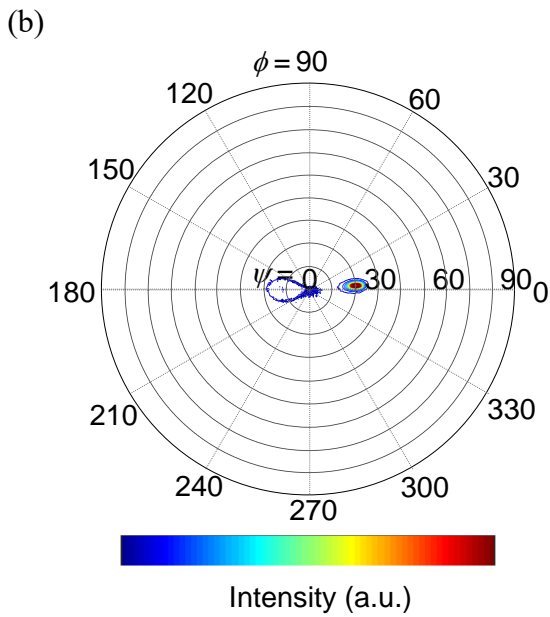


Fig. 2 (a) $(10\bar{1}1)$ pole figure of MgZnO film.
(b) (0002) pole figure of MgZnO film.

4. Electromechanical coupling coefficient

Shear wave conversion loss (CL) was measured by network analyzer (E5071C, Agilent Technologies). k'_{35^2} of MgZnO were estimated by comparing experimental CL curves with theoretical ones simulated by Mason's equivalent circuit model at thickness shear mode frequency. MgZnO thin films resonated at 250 MHz, and k'_{35^2} was estimated to be 1.3%.

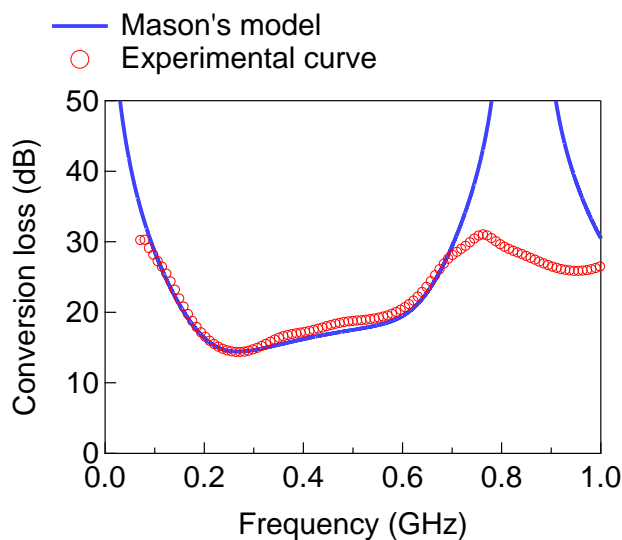


Fig. 3 Shear wave experimental and theoretical conversion loss curves of c-axis 20° tilted MgZnO epitaxial film.

5. Conclusion

The fabrication method and crystalline properties of c-axis 20° tilted MgZnO epitaxial film were reported. Estimated k'_{35^2} of 1.3% is not higher than expected from excellent crystal orientation. This may be caused by the mixing of Zn polar and O polar region.

In the future, we would like to overcome this issue.

Acknowledgement

This work was supported by JST CREST (No. JPMJCR20Q1), JST-FOREST, and KAKENHI (Grant-in-Aid for Scientific Research B, No.19H02202, No.21K18734).

References

1. J. Weber, W.M. Albers, J. Tuppurainen, M. Link, R. Gabl, W. Wersing, M. Schreite, *Sens. Actuators A.*, **128**, pp. 84-88, (2006).
2. G. Wingqvist, J. Bjurström, L. Liljeholm, V. Yantchev, I. Katardjiev, *Sens. Actuators B.*, **123**, pp. 492-495, (2007).
3. M. Link, J. Weber, M. Schreiter, W. Wersing, O. Elmazria, P. Alno, *Sens. Actuators A.*, **121**, pp. 372-378, (2006).
4. J. Wang, D. Chen, Y. Xu, W. Liu, *Sens. Actuators B.*, **190**, pp.378-383, (2014).
5. X. Zhao, G.M. Ashley, L. Garcia-Gancedo, H. Jin, J. Luo, A.J. Flewitt, J.R. Lu, *Sens. Actuators B.*, **163**, pp.242-246, (2012).
6. T. Matsuo, T. Yanagitani, M. Matsukawa, and Y. Watanabe, *Proc. IEEE Ultrason. Symp.*, pp. 1229-1232, (2007).
7. K. Izumi and T. Yanagitani, *Proc. IEEE Ultrason. Symp.*, pp. 1-3, (2020).